Characterization of the Thermotropic Behavior and Lateral Organization of Lipid-Peptide Mixtures by a Combined Experimental and Theoretical Approach: Effects of Hydrophobic Mismatch and Role of Flanking Residues

Sven Morein,*[†] J. Antoinette Killian,* and Maria Maddalena Sperotto[‡]

*Department of Biochemistry of Membranes, Utrecht University, NL-3584 CH Utrecht, The Netherlands; [†]Department of Biophysical Chemistry, University of Umeå, Umeå, Sweden; and [‡]Biocentrum-DTU, Biochemistry and Nutrition, The Technical University of Denmark, DK-2800 Kgs. Lyngby, Denmark

ABSTRACT   A combined experimental and theoretical study was performed on a series of mixtures of dipalmitoylphosphatidylcholine (DPPC) and synthetic peptides to investigate their thermotropic behavior and lateral organization. The experimental study was based on differential scanning calorimetry (DSC) and phosphorous nuclear magnetic resonance (^{31}P-NMR) techniques; the theoretical study was based on calculations on a microscopic molecular interaction model, where the lipid-peptide interaction is built on the hydrophobic matching principle. The chosen peptides, WALP and KALP, consist of a hydrophobic stretch, of variable length, of alternating leucine and alanine residues, flanked on both ends with tryptophan and lysine residues, respectively. By systematically varying the peptide hydrophobic length it was thus possible to explore different matching conditions between the peptide's hydrophobic length and the lipid bilayer hydrophobic thickness, and to investigate the potential role of flanking residues. The results show that both the WALP and the KALP peptides tend to favor the liquid-crystalline (or fluid) phase of the system; i.e., they tend to depress the main-transition temperature, T_m, of pure DPPC. However, the detailed effects of both peptides on the lateral phase behavior of the lipid-peptide system are dependent on the peptide length and the type of flanking residues. The results suggest that below T_m, the shortest among the WALP and KALP peptides induce gel-fluid phase separation in the system within an extensive temperature-composition region. The longer the hydrophobic length of the peptides is, the more narrow this region appears to become.

INTRODUCTION

The results from a number of experimental and theoretical investigations have shown that the occurrence of a mismatch between the hydrophobic length of integral membrane proteins and the hydrophobic thickness of the lipid bilayer (hydrophobic mismatch) influences the thermotropic behavior and the lateral organization of model lipid membranes (for recent reviews see Mouritsen and Sperotto, 1993; Gil et al., 1998; Killian, 1998) and might therefore be relevant for biomembrane processes such as protein translocation (de Kruijff et al., 1997), protein sorting (Bretscher and Munro, 1993; Munro, 1998), or protein enzymatic activity (Montecucco et al., 1982; Cornea and Thomas, 1994). In recent years, synthetic peptides have been used as models for the membrane-spanning part of integral membrane proteins, and a number of experiments were performed on lipid-peptide systems to quantify the consequences of hydrophobic mismatch for the phase equilibria and the lateral organization of lipid bilayers (Huschilt et al., 1985; Morrow and Davis, 1988; Zhang et al., 1992, 1995a, b; Rinia et al., 2000; Harzer

and Bechinger, 2000), and for the formation of nonbilayer structures (Killian, 1998; de Planque et al., 1998, 1999; Killian et al., 1996; Morein et al., 1997, 2000; Garab et al., 2000; Van der Wel et al., 2000; Liu et al., 2001). The hydrophobic segments of these model peptides were in most cases flanked either by tryptophans, which have been shown to interact preferentially with the interfacial region of the lipid bilayer (Persson et al., 1998; Yau et al., 1998; Killian and von Heijne, 2000), or by lysines. Both amino acids are enriched at the biomembrane-water interface in integral membrane proteins (Landolt-Marticorena et al., 1993; von Heijne, 1994; Reithmeier, 1995; Wallin et al., 1997; Ridder et al., 2000). Therefore, we thought it of interest not only to analyze mismatch-dependent effects of model peptides on the thermotropic behavior of lipid-peptide mixtures, but also to investigate whether and how these effects are influenced by the nature of the residues flanking the hydrophobic segment.

This paper presents the results of a study of the thermotropic behavior and lateral organization of mixtures of dipalmitoylphosphatidylcholine (DPPC) with different synthetic peptides. The investigation was carried out by means of differential scanning calorimetry (DSC) and phosphorous nuclear magnetic resonance (^{31}P-NMR) techniques, and it was supplemented by a theoretical study based on Monte Carlo simulation techniques on a microscopic interaction model for lipid-peptide bilayers. The chosen peptides were the WALP and KALP pep-

TABLE 1 Peptide amino acid sequence and length

Peptide	Sequence	d_P^{tot} (Å)	d_P (Å)
WALP16	Acetyl-GWW(LA)$_5$WWA-ethanolamine	24.0	21.0
WALP19	Acetyl-GWW(LA)$_6$LWWA-ethanolamine	28.5	25.5
WALP23	Acetyl-GWW(LA)$_8$LWWA-ethanolamine	34.5	31.5
WALP27	Acetyl-GWW(LA)$_{10}$LWWA-ethanolamine	40.5	37.5
KALP23	Acetyl-GKK(LA)$_8$LKKA-amide	34.5	
KALP31	Acetyl-GKK(LA)$_{12}$LKKA-amide	46.5	

Peptide amino acid sequences and peptide total and hydrophobic length estimated as follows: assuming that the peptides are α-helical, each amino acid residue contributes with 1.5 Å to the total length, d_P^{tot}, while the hydrophobic length, d_P, is estimated according to the following relation: $d_P = (n - 2) \times 1.5$ Å, where n is the total number of the amino acids in each peptide. In comparison, the calculated values of d_L for the fully melted and all-*trans* chains in DPPC are 22.5 Å and 37.5 Å, respectively (Pink et al., 1980).

tides, which have a hydrophobic core of alternating leucines and alanines residues of varying length, flanked on both ends by two tryptophan or lysine residues, respectively (Killian et al., 1996; Morein et al., 2000; de Planque et al., 1999). Both types of peptides have been shown to adopt transmembrane α-helices in a variety of lipid bilayers, including DPPC (Killian et al., 1996; de Planque et al., 1999, 2001; Rinia et al., 2001). Their amino acid sequence is given in Table 1. Previous studies on the thermotropic behavior of lipid-peptide mixtures concerned either Lys-flanked transmembrane peptides with two different hydrophobic lengths, incorporated in (perdeuterated) DPPC (Morrow at al., 1985; Lewis et al., 1987), or Lys-flanked peptides with fixed length incorporated in lipid bilayers with phospholipids with different chain lengths (Zhang et al., 1992, 1995a, b). In the present study the hydrophobic length of the peptides, and consequently the degree of hydrophobic mismatch with the DPPC bilayer thickness, is varied in a systematic manner. Moreover, the use of both WALP and KALP peptides with varying length allows a direct comparison between the effects of Trp and Lys as flanking residues on the lateral phase behavior of the lipid-peptide systems.

The results show that WALP and KALP peptides both tend to depress the main-transition temperature of pure DPPC. In addition, the results suggest that below this temperature gel-fluid phase separation may occur in the system, depending on the peptide hydrophobic length and nature of the flanking residues.

MATERIALS AND METHODS

Chemicals

DPPC was purchased from Avanti Polar Lipids, Inc. (Alabaster, AL). The purity was checked by thin layer chromatography (TLC) and the lipids were used without further purification. The WALP peptides were synthesized and purified as described elsewhere (Killian et al., 1996; Greathouse et al., 2001). The KALP peptides were synthesized as described in de Planque et al. (1999). Trifluoroacetic acid (TFA) and 2,2,2-trifluoroethanol (TFE) were obtained from Merck (Darmstadt, Germany).

Sample preparation

The lipid-peptide samples used for the DSC and NMR measurements were prepared by a mixed-film method as follows. The phospholipids (typically 5 and 20 μmol lipid for DSC and NMR experiments, respectively) were dissolved in 1.5 ml chloroform. The peptides were dissolved in TFA and dried to a film under a stream of nitrogen, and subsequently dissolved in 0.5 ml TFE. The WALP peptide concentration in stock solution was determined by the absorbance at 280 nm using an extinction coefficient of 21,300 M^{-1} cm^{-1} (Killian et al., 1996), and the KALP peptide concentration was determined on the basis of weight. Appropriate volumes of peptide stock solution and TFE, adding up to a volume of 150 μl, were added to the lipid solution. The mixture was vortexed and dried to a film under reduced pressure in a rotavapor. The samples were further dried over night under vacuum. The dry lipid film was hydrated at 45°C in a waterbath with 2 ml buffer (10 mM TRIS, 100 mM NaCl, 0.2 mM EDTA, pH 7.4). The samples used for the DSC measurements were transferred to Eppendorf tubes and centrifuged three times for 20 min at 16,000 rpm in a tabletop Eppendorf 5415 C centrifuge. Between the centrifugation steps the supernatant was removed and the peptide-lipid pellet was again dispersed in buffer. After the final centrifugation step the total volume was adjusted to get a lipid concentration of 8 mM. The washing steps were performed to remove residual traces of TFA, and hence to prevent lipid degradation. All centrifugation steps were carried out at room temperature, at which the samples were easily pelleted. From analysis of the peptide-to-lipid molar ratio (P/L ratio) in some samples after centrifugation it could be concluded that little, if any, material was lost during the centrifugation steps. Also, the DSC endotherms did not show a significant difference between washed and unwashed samples. The samples used for the NMR measurements were transferred to thick-walled 8-mm glass tubes instead of Eppendorf tubes, and were then centrifuged three times for 20 min at 15,000 rpm in an SS34 rotor with a Sorvall RC-2B centrifuge at 10°C. Between the centrifugation steps the supernatant was removed and the peptide-lipid pellet was again dispersed in buffer. After the final centrifugation step enough supernatant was left to assure that the NMR samples contained excess water. The NMR samples were freeze-thawed by subsequent freezing in an ethanol/CO$_2$(s) bath and thawing at ~50°C for at least 10 times before measurements.

In the preparation of peptide-lipid samples, TFA and TFE were used to dissolve the peptides. Pure DPPC samples prepared in the presence of these solvents showed the same thermotropic behavior as DPPC prepared in the absence of TFA and TFE.

Within the range of P/L ratios used here, all DPPC-WALP mixtures are expected to form a lamellar phase (Killian et al., 1996; de Planque et al., 1998, 1999). Using ^{31}P-NMR it was verified that also the DPPC-KALP samples at the highest P/L used (P/L = 1:25) form a lamellar phase.
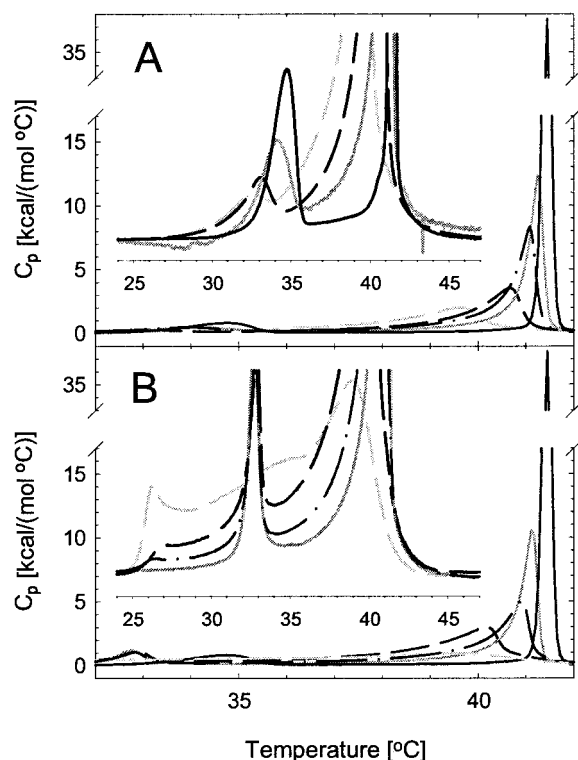
FIGURE 1 Specific heat curves corresponding to DPPC-KALP31 mixtures (*A*) and DPPC-KALP23 mixtures (*B*). The various lines refer to pure DPPC (*black*, *solid line*), and to mixtures with P/L = 1:200 (*gray*, *solid line*), 1:50 (*black*, *dashed line*), and 1:25 (*gray*, *dashed line*). The specific heats were obtained at a scan rate of 10°C/h, and are given in units of kcal/(°C mol). The insets show enlarged parts of the endotherms.

Differential scanning calorimetry

The DSC measurements were performed using an MC-2 Ultrasensitive Scanning Calorimeter from Microcal (Northampton, MA). The data shown in this paper refer to measurements done with a scan rate of 10°C/h. However, on several samples measurements were also performed with different scan rates, ranging from 30 to 1°C/h for pure DPPC, and from 30 to 5°C/h for lipid-peptide mixtures. The position of the main-transition peaks (and other peaks than the pre-transition ones) did not change significantly with scan rate, at least for scan rates equal to or below 20°C/h. For the mixed systems, the shift of the pre-transition peak position never exceeded 0.8°C. For the pure system, a large change of scan rate from 20 to 1°C/h caused a shift of, at most, 1.1°C. We are therefore confident that the systems are sufficiently equilibrated. The sample volume was 0.5 ml and the reference cell contained the same volume of buffer. To prevent bubble formation during the measurements, an additional pressure of 1 atm was applied. The reference buffer and sample were degassed by stirring in vacuum for ~20 min directly before measurements. Aliquots of sample were taken aside and the phospholipid concentration was determined by the method of Rouser et al. (1970). The baseline was corrected by subtracting the heat capacity curve from the one obtained from measurements with buffer in both DSC cells.

^{31}P-NMR spectroscopy

The ^{31}P-NMR experiments were carried out on a Bruker MSL 300 NMR spectrometer at 121.4 MHz, with a 17-μs 90° pulse, a 1.3-s interpulse time, and gated proton-noise decoupling. A 100-Hz line broadening was applied before Fourier transformation. For each chosen temperature, the samples were allowed to equilibrate for 1 h before recording the spectra.

Microscopic model

The theoretical model, used to describe a lipid bilayer with incorporated transmembrane peptide-like impurities (Sperotto, 1997), is built on the 10-state Pink model (Pink et al., 1980) to account for the gel-fluid transition of pure DPPC lipid bilayer in the fully hydrated state. The 10-state model was successful in predicting and describing thermodynamic, thermomechanic, and spectroscopic data for a variety of phospholipid membranes (Mouritsen, 1990; Mouritsen et al., 1995). It is a pseudo-two-dimensional lattice model that neglects the translational modes of the lipid molecules and focuses on the conformational degrees of freedom of the acyl chains and their mutual interactions and statistics. The bilayer is considered as two independent monolayers, each represented by a triangular lattice on which the lipid chains are arrayed, one chain at each site. Each lipid acyl chain can take on one of ten conformational states, each of which is characterized by a hydrocarbon chain length. Within the lattice formulation, a peptide-like molecule occupies seven lattice sites, and its hydrophobic part is assumed to be smooth, rod-like, and defined only by a cross-sectional area and a hydrophobic length, d_P. The lipid-protein interactions were incorporated into the model in the spirit of the phenomenological mattress model of lipid-protein interactions in membranes (Mouritsen and Bloom, 1984), which is formulated in terms of an attractive van der Waals-like interaction between peptide and lipids, and a repulsive interaction due to mismatch between the hydrophobic thickness of the lipid bilayer, d_L, and d_P.

Model parameters

The values of the lipid-protein interaction parameters were estimated from the experimental specific heat data referring to the DPPC-WALP23 mixtures. Their value has been chosen to reproduce qualitatively, by a phenomenological best-fitting, the dependence on P/L of the main-transition peak, i.e., change in peak position, broadening, and intensity. The results from the model study were then used to make predictions for the thermodynamic quantities referring to the lipid-peptide mixtures with the other WALP peptides. One reason why the WALP peptides, rather than the KALP peptides, were chosen as model peptides is that four types of homologous WALP peptides, WALP16, WALP19, WALP23, and WALP27, were used during the experimental study, while only two types of KALP peptides, KALP23 and KALP31, could be considered, due to the high water solubility of shorter KALP peptides.

Because the peptide hydrophobic length is a model input parameter whose value had to be estimated a priori, the choice for WALP peptides as model peptides was furthermore motivated by the fact that it is more straightforward to give an estimate for the values of d_P of WALP peptides than for d_P values of KALP, for the latter will be biased by the "snorkeling" behavior of the aliphatic side chains of the lysines (Segrest et al., 1990; de Planque et al., 1999). Assuming that the peptides are α-helical, each amino acid residue contributes with 1.5 Å to the peptide total length, d_P^{tot}. Considering that the Trp side chain localizes near the carbonyl region (Persson et al., 1998; Yau et al., 1998; de Planque et al., 1999), it seems reasonable to estimate the hydrophobic length of the WALP peptides from the positions of these residues. The values of d_P were thus calculated according to the following relation: $d_P = (n - 2) \times 1.5$ Å, where n is the total number of the amino acids in each peptide (see Table 1). These values

are given in Table 1 together with the estimated values of d_P^{tot}. In comparison, according to the Pink model (Pink et al., 1980), the calculated values of d_L for the fully melted and all-*trans* chains in DPPC are 22.5 Å and 37.5 Å, respectively.

Computational techniques

The thermodynamic properties of the model were calculated by standard Metropolis Monte Carlo simulation techniques (Mouritsen, 1990) on a lattice with a fixed number of sites, under conditions of constant temperature and surface pressure. The advantage of using these techniques is that it is possible to inspect the lipid bilayer configuration at the molecular level, and thus to provide its lateral organization. Most of the simulations were done in the Canonical ensemble, where the number of peptide molecules, i.e., the P/L, is fixed. In a few cases, simulations were done in the Grand Canonical ensemble where the number of peptide molecules, i.e., the composition of the system, is let to fluctuate over the micro-configuration of the equilibrium ensemble, depending on a fixed parameter representing the difference in chemical potential of the lipid chains and peptides, thus allowing the system to sample between possible coexisting macroscopic phases (Zhang et al., 1993). Simulations in this ensemble were needed to establish whether what seems to be a phase separation between two phases, based on snapshots of typical micro-configurations of the mixture, really is a phase separation into two macroscopic equilibrium phases, or merely the onset of metastable non-equilibrium phases.

The thermal equilibrium was achieved by a combination of Glauber and Kawasaki dynamics. The Monte Carlo method with Glauber dynamics was used for the single-chain conformational excitations regarding the internal transition between two of the ten possible conformational states of the acyl chains (simulations in the Canonical ensemble), and for the conversion of a seven-site peptide into seven lipid chains with simultaneous assignment of random acyl chain conformations, or for the conversion of adjacent seven chains, corresponding to a seven-site hexagon, into a peptide molecule (simulations in the Grand Canonical ensemble). The Kawasaki dynamics was used in the Canonical ensemble for the lipid and peptide diffusive exchange.

To gain access to the bulk thermodynamic state of the mixtures in equilibrium, the specific heat per lipid molecule, C_P, was calculated together with the mean hydrophobic thickness of the lipid bilayer, d_L. To characterize the peptide lateral distribution, the equilibrium probability of finding a cluster of n peptide monomers ($n = 1, 2, \ldots$) was calculated (Sperotto, 1997) and compared with the one of a mixture with a truly random distribution of peptides, i.e., for a system at an infinitely high temperature. The simulations were performed on a triangular lattice of 40×40 sites (Canonical ensemble). Each system was equilibrated at least for 40,000 Monte Carlo steps per site, and statistical averages were then calculated over 40,000 equilibrium configurations, each of which is "separated" by five Monte Carlo steps per site. The data discussed below refer to P/L = 1:100 and 1:66.

RESULTS

DSC

The thermotropic behavior of the various peptide/lipid systems was first investigated by DSC. Measurements were performed on pure DPPC, on DPPC-WALP, and on DPPC-KALP mixtures with a P/L in the range of 1:500–1:25. Typical endotherms are shown in Figs. 1 and 2. The values of the temperatures corresponding to the maximum of the thermal anomalies appearing in the different endotherms are listed in Table 2.
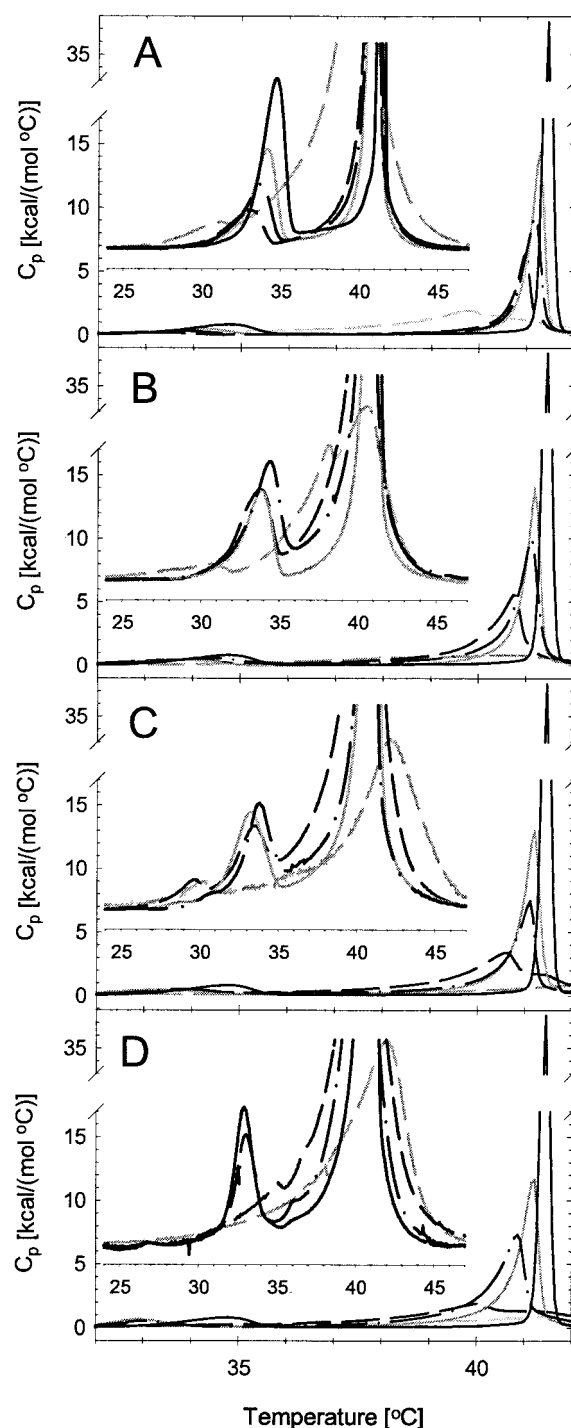
FIGURE 2 Specific heat curves corresponding to DPPC-WALP27 mixtures (*A*), DPPC-WALP23 mixtures (*B*), DPPC-WALP19 mixtures (*C*), and DPPC-WALP16 mixtures (*D*). The various lines refer to pure DPPC (*black*, *solid line*), and to mixtures with P/L = 1:200 (*gray*, *solid line*), 1:50 (*black*, *dashed line*), and 1:25 (*gray*, *dashed line*). The specific heats were obtained at a scan rate of 10°C/h, and are given in units of kcal/(°C mol). The insets show enlarged parts of the endotherms.

For pure DPPC, the endotherm (see, e.g., Fig. 1 *A*) shows two thermal anomalies: a peak having a maximum located

TABLE 2 Transition temperatures

	T_-	T_m	T_+	T_p
DPPC		41.4		34.7
KALP31/DPPC				
1:200		41.2		34.0
1:100		41.1		33.9
1:50		40.5		33.0
1:25		39.6		32.7
KALP23/DPPC				
1:500		41.3		32.8
1:300		41.3		32.5
1:200	25.7	41.1		32.7
1:100	26.3	40.9		32.8
1:67	26.7	40.6		32.9
1:50	26.2	39.7		32.8
1:25	26.3	38.9		—
WALP16/DPPC				
1:300		41.3		33.5
1:200		41.2		32.9
1:100		40.9		32.9
1:67		40.4		—
1:50	35.0	40.0	41.1	—
1:35		41.3		—
1:25		42.0		—
WALP19/DPPC				
1:300		41.2		33.4
1:200	29.0	41.2		33.4
1:100	30.6	41.1		33.8
1:67	30.7	40.8		33.9
1:50	30.8	40.4	41.2	33.7
1:25	30.3	42.2		—
WALP23/DPPC				
1:300		41.3		34.1
1:200		41.2		33.8
1:100		41.1		34.3
1:50		40.7		33.8
1:25	30.8	40.6	38.1	—
WALP27/DPPC				
1:300		41.3		34.3
1:200		41.3		34.2
1:100		41.2		33.8
1:50		41.0		33.2
1:25	31.1	39.8	40.5	—

Temperatures, in °C, corresponding to the maximum of the main transition peak (T_m) and of the pretransition peaks (T_p), as a function of peptide type, and P/L. The main transition peak is defined as the peak with the highest maximum in the vicinity of T_m of the pure lipid. The temperatures related to other thermal anomalies are listed under the T_- or T_+ column, in case they appear below or above the one listed under T_m, respectively.

at 34.7°C and a larger peak with a maximum at 41.4°C. For these peaks transition enthalpies were calculated of 1.4 and 9.0 kcal/mol, respectively. The two thermal anomalies correspond to the pre-transition (from the gel phase, $L_{\beta'}$, to the gel ripple phase, $P_{\beta'}$) and the main-transition (from $P_{\beta'}$ to the liquid-crystalline, or fluid, phase, L_α) temperatures, T_p and T_m, respectively. The values found for the transition temperatures are in accordance with other published data (Lewis et al., 1987; Silvius, 1982).

For both KALP and WALP peptides, the thermotropic behavior of the peptide/lipid mixtures is strongly dependent on the peptide length as well as on the P/L ratio, as shown in Figs. 1 and 2, respectively. The thermograms for the different peptides as function of peptide concentration will now be discussed for each peptide separately.

As shown in Fig. 1 *A*, incorporation of KALP31 leads to a shift of the position of the maximum and a broadening of both the pre- and the main-transition peaks of pure DPPC, which becomes more pronounced with increasing P/L ratio. Also, the temperature maxima of both the main and pre-transition gradually decrease with increasing P/L (Table 2). Similar trends were observed when lysine-flanked synthetic transmembrane peptides were incorporated into DPPC bilayers (Lewis et al., 1987; Zhang et al., 1992, 1995b). The thermograms of DPPC-KALP23 shown in Fig. 1 *B* look quite different from the ones of DPPC-KALP31. At least for P/L ≥ 1:200, each of the specific heat curves related to DPPC-KALP23 mixtures has three thermal anomalies. The first peak has a maximum located at a temperature close to T_m. As found for KALP31, this peak broadens as P/L increases and the position of its maximum gradually decreases (Table 2). The second peak, which is related to the pre-transition, has a maximum located around 33°C independent of P/L, until the pre-transition completely disappears at a P/L of 1:25 (see also Table 2). The third peak has a lower intensity than the first one, and a maximum which remains located around 26°C when P/L increases. Furthermore, the intensity of the specific heat "in between" the first and third peak increases as P/L increases. These data suggest that, below T_m and depending on P/L, gel-fluid phase separation may occur in the system, as argued in the section "Phase diagram of DPPC-KALP23." Mixtures with lysine-flanked peptides shorter than KALP23 peptides were not investigated by DSC, as these peptides are not sufficiently hydrophobic to incorporate into a DPPC lipid bilayer, and remain instead in the buffer solution (de Planque et al., 1999). Thus, although both the lysine-flanked KALP23 and KALP31 peptides depress the main-transition temperature of pure DPPC, namely favor the fluid phase of the system, they nevertheless have markedly distinct effects on the thermotropic behavior of the system.

Incorporation of the WALP peptides into DPPC causes a concentration-dependent broadening of the pre- and main-transition peaks, as well as a shift toward lower temperatures of their peak maxima, at least for P/L up to 1:50 (see Fig. 2, *A*--*D*). The results in Fig. 2 and Table 2 suggest that the shorter peptides are only slightly more effective than the longer peptides to lower the position of their main-transition peak maximum, at least for P/L above 1:300 and up to 1:50. In addition, the shorter the peptides are, the more pronounced their effect is in broadening the main-transition peak. This is qualitatively similar to what was observed for the KALP peptides. Furthermore, for all WALP peptides, at high P/L a shoulder appears on the side of the peak associated with the main-transition. This feature is not detectable in any of
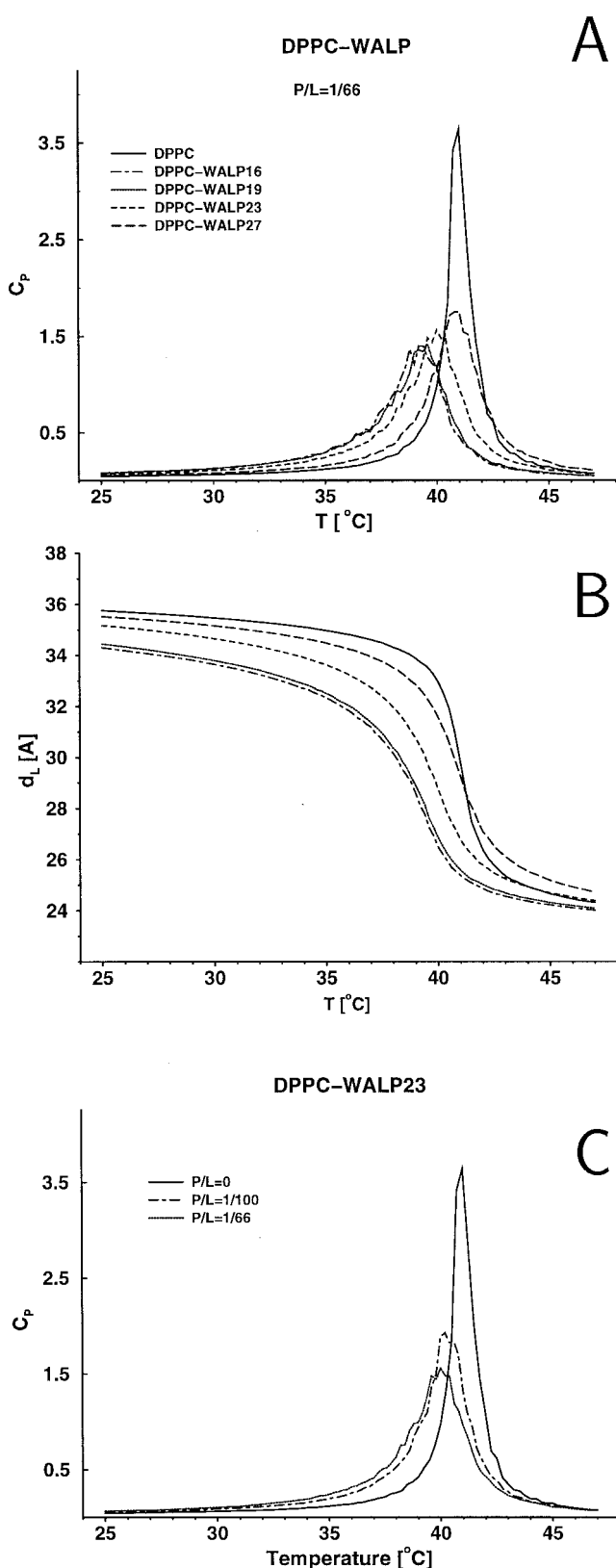
DPPC–WALP

P/L=1/66

the DPPC-KALP systems. Depending on P/L and on the hydrophobic length of the peptides, such a thermal anomaly can turn into a peak, and can extend to both sides of the main-transition temperature of pure DPPC. In particular, in the case of WALP16, at around P/L = 1:67 (data not shown) a broad shoulder appears at the high-temperature side of the main-transition peak that then develops into a peak at P/L = 1:50 (Fig. 2 *D*). At P/L = 1:25 only one dominating feature remains in the endotherm, namely a broad peak, which extends to both sides of T_m (compare the thermogram for pure DPPC in Fig. 2 *A*), and has a maximum located at a temperature higher than T_m. Another anomaly with a very low intensity is detectable around 35°C at P/L = 1:100 (data not shown), and is present also when P/L is up to 1:50 (see Table 2). In the case of the DPPC-WALP19 system (Fig. 2 *C*), at P/L = 1:50 a shoulder also forms at the high-temperature side of the main-transition peak, and its intensity increases as P/L increases. As in the endotherm of DPPC-WALP16, at P/L = 1:25 only one main thermal anomaly remains in the endotherm that extends to both sides of T_m, and has a maximum that correspond to a temperature higher than T_m. The appearance of another shoulder/peak close to the main-transition peak is also observed in the endotherms of the systems with longer WALP23 (Fig. 2 *B*) and WALP27 (Fig. 2 *A*) peptides, but at a higher P/L than in the case of the systems with WALP16 and WALP19 (see Table 2).

The endotherms of DPPC-WALP19 show yet another thermal anomaly, characterized by a low intensity, which starts to appears at P/L = 1:200 and remains at higher P/L. Its maximum is located around 30°C independent of the peptide concentration. An anomaly at the same temperature is not present in the mixtures with WALP16, nor in the mixtures with KALP23 and KALP31, while it appears in both the DPPC-WALP23 and DPPC-WALP27 mixtures with P/L = 1:25.

Regarding the pre-transition temperature and its dependence on P/L (Table 2), incorporation of WALP16 and WALP19 already at a P/L ratio of 1:300 leads to an initial lowering of the pre-transition temperature as compared to pure DPPC, which then remains relatively constant when P/L increases further. In the case of WALP16, for mixtures with P/L = 1:67 or higher, the pre-transition peak can no longer be observed. For WALP19, WALP23, and WALP27 the pre-transition peak disappears at a higher P/L of 1:25. For WALP27 the value of the pre-transition temperature appears to gradually decrease as P/L increases, as can be seen from Table 2.

DPPC–WALP23

FIGURE 3 Calculated specific heat curves (*A*) and mean lipid bilayer hydrophobic thickness (*B*) corresponding to pure DPPC (——), DPPC-WALP27 (− − −), DPPC-WALP23 (- - -), DPPC-WALP19 (·········), and DPPC-WALP16 (−· − · −) model mixtures with P/L = 1:66. Calculated specific heat curves (*C*) corresponding to pure DPPC (——) and to DPPC-WALP23 model mixtures with P/L = 1:100 (− − −) and 1:66 (·········). The specific heats are given per lipid molecule, and in units of 10^{-13} erg/K.

Model

Fig. 3 *A* shows the calculated specific heat curves, C_P, for pure DPPC lipid bilayers and for lipid-peptide mixtures with the four homologous model WALP peptides. The results refer to a P/L = 1:66. The calculated C_P for the pure system has a peak with a maximum located at 41°C, which corresponds to the main-transition temperature. When the peptides are present in the lipid bilayer they induce a broadening of the transition peak and a shift of the position of the peak maximum toward temperatures below T_m. The shorter the peptides are, the more pronounced the shift is. Furthermore, for each lipid-peptide mixture, the C_P peak intensity is lower than the intensity of the C_P peak of the pure DPPC lipid bilayer, and it decreases by decreasing the peptide hydrophobic length. For lipid-peptide mixtures containing the same type of peptides, but with varying values of P/L, both the intensity of the specific heat peaks and the temperatures corresponding to the position of the peak maximum decrease as P/L increases. In particular, Fig. 3 *C* shows the results related to DPPC-WALP23. Thus, the results obtained by computational methods are qualitatively consistent with the experimental results discussed previously and summarized in Table 2.

Fig. 3 *B* shows the calculated mean lipid bilayer hydrophobic thickness, d_L, as a function of temperature for the various systems. Above T_m the mixtures are in the fluid phase because the d_L values are close to those of the pure system in the fluid phase, although the longer peptides have the tendency to thicken slightly the pure lipid bilayer, while the shorter peptides have the opposite effect. This is qualitatively in agreement with ^{2}H-NMR results on DPPC-WALP mixtures (de Planque et al., 1998). Below T_m all peptides cause a thinning of the bilayer, the shortest peptides causing the strongest effects. From the theoretical calculations it is possible to inspect the bilayer on a microscopic level. Fig. 4 shows the snapshots from typical micro-configurations of pure DPPC and of DPPC-WALP with P/L = 1:66. The left column refers to 38°C ($<T_m$), while the right column refers to 44°C ($>T_m$). The statistical analysis of the state of aggregation/dispersion of the peptides (data not shown) confirms what can be seen from the snapshots from typical micro-configurations of the mixtures with P/L = 1:66. At this P/L, and above T_m, the peptides have a lateral distribution similar to that of a random distribution. At 38°C, the lateral structures of the mixtures differ markedly from one another depending on the hydrophobic length of the peptides considered. Compared to pure DPPC, the mixture with the shorter WALP16 peptides seems to separate into two regions, a peptide-free gel region and an extended fluid region into which the peptides tend to segregate. To make sure that these "regions" correspond to macroscopic equilibrium phases, simulations have been done in the Grand Canonical ensemble. The value of the internal energy of the system (order parameter) was moni-

tored as a function of the simulation time. The results (not shown) from these simulations indicate that what is shown in the micro-configurations reflects the fact that at 38°C the system phase-separates into two macroscopic phases, a fluid phase enriched in peptides, having a P/L of ~1:21, and a gel phase with a very low peptide concentration (P/L < 1:1500). The longer the peptides are, the less extended the fluid phase appears, and in the case of the longest peptide, WALP27, the lipid-peptide mixture at 38°C appears to be completely in the gel phase, where the peptides are randomly dispersed. This suggests that the longer the peptides are, the more narrow is the temperature-composition region within which the system phase-separates.

^{31}P-NMR

^{31}P-NMR measurements were performed on selected DPPC-peptide systems to gain further insight into the effect of the peptides on the state of the phospholipids. Only lipid-peptide mixtures with the shortest peptides, KALP23 and WALP16, were investigated, because the DSC results and the theoretical data (the latter concerning the WALP peptides) suggested that, below T_m, these peptides induce lateral gel-fluid phase separation in the mixed systems. According to the lever-rule, for a fixed temperature and at low P/L (within the phase-separation range), the predominant phase in the system is the gel phase, which would be present anyway below T_m in non-separated mixtures. Therefore, reasonably high values of P/L of 1:67 were considered to make sure that there was enough fluid phase to be detected with ^{31}P-NMR spectrometry. In the case of WALP peptides, this value corresponds to the one used for the theoretical study. The results from the ^{31}P-NMR measurements on pure DPPC, on DPPC-WALP16, and on DPPC-KALP23 mixtures, are shown in Fig. 5, *A–C*, respectively.

The ^{31}P-NMR spectrum of pure DPPC (Fig. 5 *A*) at 30°C ($<T_m$) shows features that are characteristic for phospholipids in a bilayer in the gel state, i.e., a large chemical shift anisotropy (csa) and a broad line with an overall high intensity, indicative of a slow motion of the phosphate group. As the temperature increases, the csa decreases and the lineshapes of the spectra get sharper, probably due to an increase in the motion of the phosphatidylcholine headgroups (Seelig, 1978; Lindblom, 1996). At 41°C the ^{31}P-NMR spectrum is characteristic for phospholipids in the L_α phase. As the temperature is increased to 50°C, no significant changes are observed in the lineshapes of the spectra compared to the ones shown at 41°C (not shown).

In Fig. 5 *B* ^{31}P-NMR spectra are shown of a DPPC-WALP16 sample with P/L = 1:67. The spectra recorded at 30°C and 35°C show features that are typical for a phospholipid bilayer in the gel state. In the spectrum obtained at 37°C two overlapping components can be observed, one typical for molecules in a gel state, and another related to molecules in a fluid state. This is in contrast to the situation
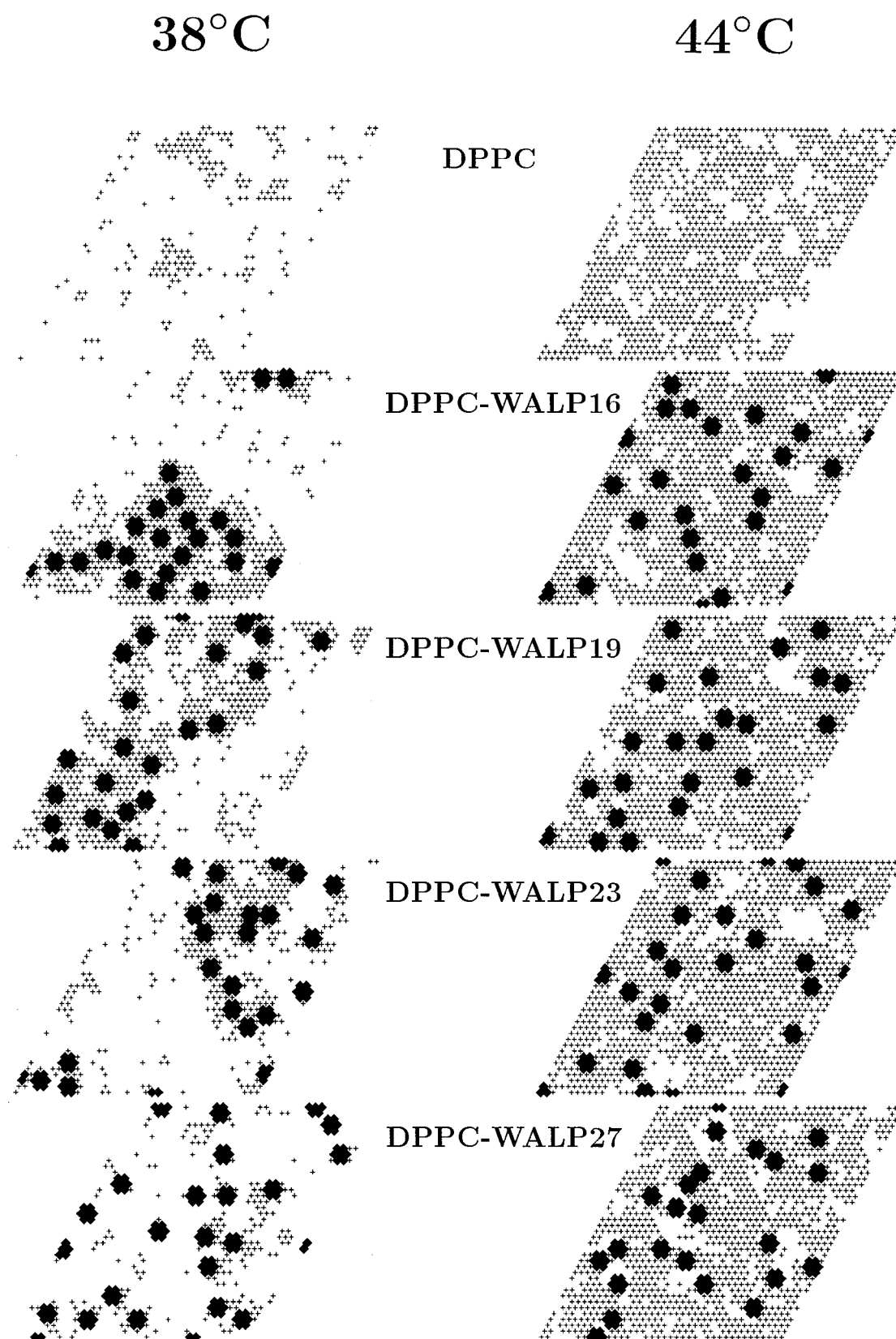
38°C   44°C

FIGURE 4   Snapshots from typical micro-configurations at 38°C (*left column*) and 44°C (*right column*) corresponding to pure DPPC and to DPPC-WALP mixtures with P/L = 1:66. The symbols indicate the following: ● = peptide segment, × = fluid DPPC, no symbol = gel DPPC.
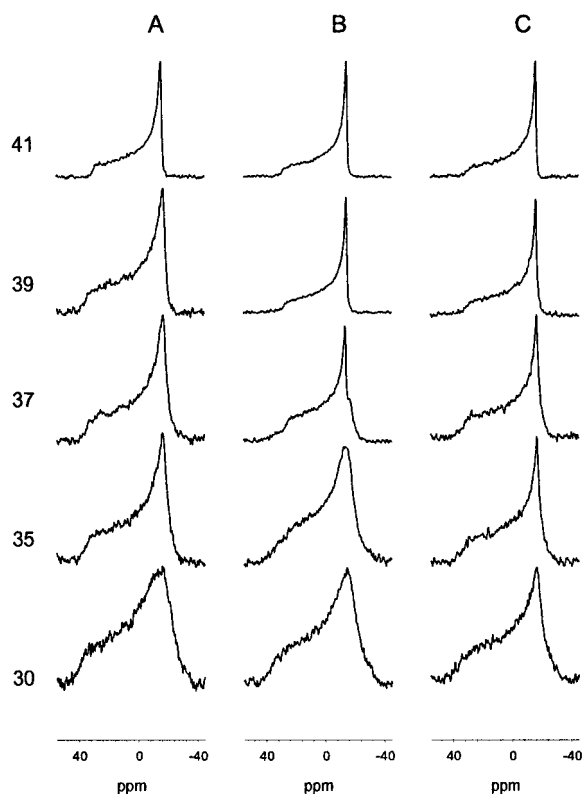
FIGURE 5 ^{31}P-NMR spectra recorded at different temperatures and corresponding to pure DPPC (*A*), DPPC-WALP16 (*B*), and DPPC-KALP23 (*C*) mixtures with P/L = 1:67.

for the pure lipids, which at 37°C are still in a gel phase. The results suggest that, at this P/L, the mixture might phase-separate into a peptide-enriched L_α-phase and a peptide-depleted gel phase. At 39°C, the lineshape of the spectrum indicates that the majority of the lipids are now in the fluid phase. Qualitatively similar behavior is observed in the presence of KALP23 at the same P/L and approximately the same temperature (Fig. 5 *C*). Thus, the spectral shapes in the presence of WALP16 and KALP23 confirm that these peptides tend to depress the main-transition temperature and suggest that they may induce gel-fluid phase separation below T_m.

Phase diagram of DPPC-KALP23

From the experimental data it is possible to construct an approximate temperature-composition (*T*, P/L), phase diagram of DPPC incorporated with the shorter of the KALP peptides, KALP23. The phase diagrams of the other systems will only be qualitatively outlined, based on the combined experimental and theoretical results. One should bear in mind that it is difficult to obtain accurate phase diagrams without having access to the free energy of the system, but only to its derivatives, as specific heats or spectroscopic order parameters. Neither the appearance of anomalies in

the specific heat alone is a sufficient condition for the existence of phase boundaries (Zhang et al., 1993), nor the superposition of two different components in a spectroscopic curve alone is sufficient to imply that two thermodynamic phases are present in a mixture. Furthermore, the conclusions, which are drawn below about the location of possible phase boundaries in the (*T*, P/L) phase diagram, are based on the endotherm peak position of what are assumed to be fully equilibrated systems. It has recently been shown that phase-separated binary lipid systems need at least 1 h to reach full equilibrium (Jørgensen et al., 2000). Therefore, to be completely sure that a system is fully equilibrated, techniques other than DSC should be applied (Jørgensen et al., 2000; Loura et al., 2000). Anyway, just by using DSC it will not be possible to distinguish between, for example, the formation of two macroscopic well-separated gel and fluid phases (raising from complete equilibrium), or "phases" made of interconnected gel and fluid macro-domains, which appear before the system is fully equilibrated, as Jørgensen et al. have detected. Therefore, what is shown and discussed below concerning (*T*, P/L) phase diagrams is only meant to be a guideline for future investigations. More experimental data, and other types of experimental techniques than those adopted during this study, are needed to provide exact phase diagrams for DPPC-KALP23 and the other systems investigated here.

Fig. 6 shows the tentative (*T*, P/L) phase diagram for DPPC-KALP23. For each P/L value the dots are derived from the temperature values that correspond to the maximum of the specific heat thermal anomalies, while the lines indicate possible phase boundaries. The shape of the endotherms shown in Fig. 1 *B* suggest that, below T_m and above 26°C, there is a broad P/L range within which the system undergoes a phase separation between a peptide-depleted gel phase and peptide-enriched fluid phases. The suggestion is based upon the following observations: 1) the temperature associated with the maximum of the pre-transition peak does not change significantly by changing P/L, at least for P/L $\geq$ 1:500. If a mixture does not phase-separate, but remains in a one-phase region, one may instead expect that the pre-transition temperature changes by changing P/L, as it is indeed observed in the case of mixtures with KALP31 and WALP27 (see Table 2); 2) the intensity between the two specific heat peaks not related to the pre-transition increases as the P/L ratio increases, suggesting that the liquidus (gel-fluid to fluid) phase line varies very slowly upon changing temperature, and therefore its slope is much lower than the slope of the solidus (gel to gel-fluid) phase line, which lies "close" to the temperature axis. Therefore, at 30°C and P/L = 1:67, one would expect that, according to the lever rule, little of the fluid phase is present and most of the system is in the gel phase. This is indeed consistent with what is suggested from the ^{31}P-NMR results obtained at the same temperature and P/L value. Vice versa, at approximately the same temperature but higher P/L = 1:25,
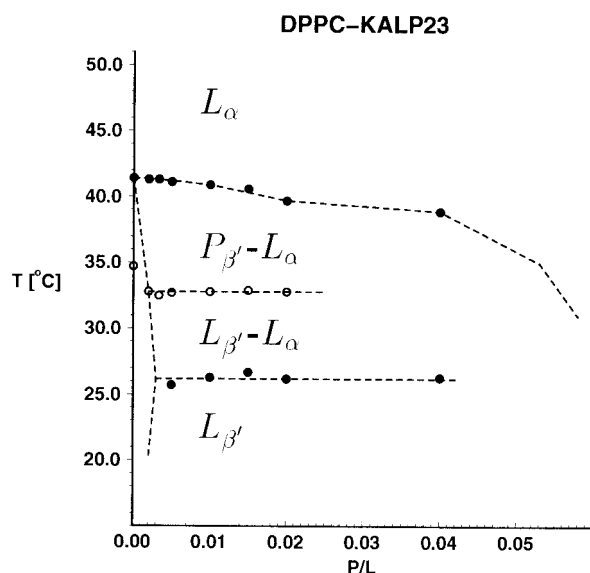
DPPC–KALP23

FIGURE 6   Suggested temperature-composition phase diagrams for the DPPC-KALP23 system. For each P/L ratio the dots are derived from the temperatures corresponding to the maximum of the specific heats thermal anomalies. The lines are suggested phase boundaries.

one would expect that most of the system is in the fluid phase and only a small amount of gel phase is present. This is consistent with ^{31}P-NMR results at this P/L ratio (not shown). Below 26°C, these ^{31}P-NMR measurements were indicative for the system being in the gel phase. Therefore, the horizontal phase line at ~26°C marks a possible transition between gel phase(s) (for example, two coexisting $L_{\beta'}$ phases characterized by two different P/L ratios), and between the $L_{\beta'}$ phase coexisting with the fluid phase. The horizontal phase line at ~33°C marks what could be a possible transition between the $L_{\beta'}$ phase coexisting with the L_{α} phase, and the $P_{\beta'}$ phase coexisting with the L_{α} phase.

The thermograms of DPPC incorporated with the long lysine-flanked peptides KALP31 look quite different from the one of DPPC with KALP23, and resembles more the one of DPPC with WALP23. We will now discuss the tentative phase diagrams of the different WALP peptides, starting with the shortest peptide, WALP16. Consistent with the theoretical predictions, the results from the ^{31}P-NMR investigation suggest that, below T_m and above T_p, the DPPC-WALP16 mixtures (P/L = 1:67) undergo a gel-fluid phase separation. Because below T_p the system is in the gel phase, one might then expect that the solidus line lies above T_p. The simulation data related to the other homologous WALP peptides suggested that the longer the peptides are, the more narrow the gel-fluid phase separation becomes, consistent with the fact that the long WALP peptides would favor less the fluid phase than the shorter ones do. Therefore one may argue that, at least for P/L up to 1:67, the temperature-composition phase diagram of DPPC incorporated with

KALP31, WALP23, and WALP27 are characterized by a more narrow gel-fluid phase separation region than the one related to the DPPC-KALP23 system. Because the variation of the main transition temperatures as a function of P/L resembles one another in all these systems, one may expect that each of the liquidus lines of the three former systems is located approximately at the same temperature-composition position as the liquidus line of the DPPC-KALP23 system. The slope of the solidus line in each of the three systems depends on the peptide length (the longer the peptide, the lower the slope), and one may expect that in all cases this slope is lower than the one of the solidus line of DPPC-KALP23, which in turn is lower than the slope of the solidus line of DPPC-WALP16.

DISCUSSION AND CONCLUSIONS

The existence of a hydrophobic mismatch, and the presence of specific types of residues flanking the hydrophobic stretch of the peptides, result in both systematic and non-systematic effects on the cooperative behavior, hence the thermotropic behavior and lateral organization of the DPPC-WALP and DPPC-KALP systems.

There is, however, one motif that is common to these and other lipid-peptide systems with transmembrane peptides (see, e.g., Morrow et al., 1985; Morrow and Davis, 1988; Zhang et al., 1995b), and does not depend on the amino acid sequence or the length of the peptide's hydrophobic part or the type of flanking residues: the presence of peptides tends to depress the melting temperature of pure lipid bilayer, i.e., the peptides tend to favor the fluid phase of the system. The DSC results shown here demonstrate that even the long peptides, WALP27 and KALP31, do not favor the gel phase. Nevertheless, the mattress model (Mouritsen and Bloom, 1984) predicted that in the case of positive mismatch (i.e., $d_P > d_L^*$, where d_L^* is the average between the lipid bilayer hydrophobic thickness in the gel and in the fully melted state), the solidus (gel to gel-fluid) and liquidus (gel-fluid to fluid) phase lines should appear at a temperature higher than the melting temperature of the pure lipid system, i.e., that the presence of the proteins should favor the gel phase. This has indeed been observed for large transmembrane proteins reconstituted into phospholipid bilayers (Peschke et al., 1987; Riegler and Möhwald, 1986; Morrow et al., 1986), in agreement with the mattress model quantitative predictions (Sperotto and Mouritsen, 1988; Sperotto et al., 1989). One possible explanation is that in contrast to what happens for bulky, multi-spanning transmembrane proteins, for long ($d_P > d_L^*$) but nevertheless "skinny" single-spanning transmembrane peptides it might be energetically more favorable to undergo transformations (such as tilting or backbone adaptations), thereby favoring the bilayer fluid phase, rather than to stabilize a bilayer gel phase above the melting temperature of the pure lipid bilayer. Recent spectroscopic studies (de Planque et al., 2001)

suggest that neither tilting nor backbone adaptations are particularly favorable reactions of these peptides to hydrophobic mismatch. Hence, such adaptations may be even less favorable in larger membrane proteins, where interactions with neighboring helices may be more important for determining the preferred tilt than interactions with the surrounding lipid bilayer.

An alternative response of a peptide/lipid system under extreme mismatch conditions is that long peptides may avoid incorporation into the lipid bilayer. Long peptides can be expelled from thin fluid lipid bilayers and form instead undefined peptide-rich aggregates with part of the lipids (de Planque et al., 2001; Morein et al., 2000). Therefore, it is possible that the long WALP27 does not completely incorporate into fluid DPPC, and the effective P/L ratio in the bilayer might be slightly different from the global one.

The peptides used for the present study also cause specific, non-trivial effects on the cooperative behavior of the system. For example, at high peptide concentrations, in the DPPC-WALP systems a thermal anomaly occurs near to the main-transition peak. Especially for the shorter WALP peptides, and at high peptide concentrations, it may extend to both sides of the main-transition temperature of pure DPPC. This type of anomaly is neither present in the endotherms of the DPPC-KALP system, at least at the P/L used in this investigation, nor in the endotherms from the mixtures of DPPC and a similar lysine-flanked peptide, KK(LA)12KK (Zhang et al., 1995b), although much higher P/L values were considered than in the present work. Broad thermal anomalies were also observed in endotherms from DPPC with incorporated lysine-flanked poly-leucine peptides (Morrow et al., 1985; Zhang et al., 1993) and from DPPC and dimyristoylphosphatidylcholine (DMPC) incorporated with gramicidin A, a tryptophan-flanked peptide (Datema et al., 1986; Morrow and Davis, 1988; Kobayashi and Fukada, 1998; Killian and de Kruijff., 1985), suggesting that their appearance does not originate from specific lipid-tryptophan or lipid-lysine interactions. Thus, this broad thermal component could be due to the presence of a phase transition. Shoulder-like anomalies have also been observed in the endotherms of DPPC-cholesterol mixtures (Vist and Davis, 1990) and have been attributed to the appearance of the so-called liquid-ordered phase, where the lipids are characterized by highly ordered acyl chains, although their lateral and rotational diffusion is comparable to that of molecules in the liquid-crystalline state (Vist and Davis, 1990). However, no chain-ordering effect was found for the DPPC-WALP16 system above T_m (de Planque et al., 1998). Therefore, the appearance of shoulders in the endotherms of lipid-peptide systems must originate from other physical mechanisms than the ones connected to the dual molecular nature of the cholesterol molecules (Ipsen et al., 1987). Another possible explanation for the anomalies in the DPPC-WALP systems is provided by the results from theoretical studies on lipid-peptide mixtures (Zhang et al.,

1993). These studies showed that the existence of a broad specific heat thermal anomaly, which persists beyond the liquidus phase line, does not necessarily correspond to a transition enthalpy, but may be due the existence of a critical mixing point in which vicinity density fluctuations are strongly enhanced, thus giving a thermal contribution to the specific heat.

The results from the present study suggest that the lateral phase behavior of DPPC-KALP23 is characterized by having an extensive region below T_m within which the system undergoes a gel-fluid phase separation (see Fig. 6), and that also the much shorter WALP16 peptides cause gel-fluid phase separation below T_m. The results from previous investigations (de Planque et al., 1999, 2001), obtained at temperatures above the melting temperature of the pure lipid system (i.e., in the fluid phase) show that the KALP peptides behave like they are effectively shorter than corresponding WALP peptides, at least concerning their effects on lipid phase behavior and lipid acyl chain ordering. Thus, one may be tempted to ascribe the similarity between the effects of KALP23 and WALP16 on DPPC to a similarity in effective hydrophobic length. However, the phase behavior of the DPPC-WALP16 system seems altogether different from the one of the DPPC-KALP23 system; therefore, not only the peptide hydrophobic length and the nature of the flanking residues, but also the chosen temperature and bilayer composition of the system have to be considered when one wants to investigate the effect of peptides on the lipid physical state.

Investigations based on atomic force microscopy technique (AFM) have recently been made at room temperature to visualize the lateral structure of DPPC-WALP and DPPC-KALP bilayers with various P/L (Rinia et al., 2000, 2001). Opposite to what happens for the DPPC-KALP systems, the DPPC-WALP systems are all characterized by having striated areas, which form in the bulk, $L_{\beta'}$ phase, and whose extent and detailed appearance depend on d_P and P/L. The striated appearance is attributed to a kind of modulated structure induced by the alignment of the peptides along rows that are intercalated by lipid molecules. It is not clear whether or not these areas constitute a macroscopic equilibrium phase. However, if so, the thermal anomaly found in all the endotherms of DPPC-WALP19 at ~30°C could indicate a possible transition between a $L_{\beta'}$ phase and another phase(s) characterized by the striated "phase" in equilibrium with the $L_{\beta'}$ phase. Interestingly, a transition around 30°C has also been detected by DSC in multilamellar DPPC liposomes mixed with the acylated cationic decapeptides (myristoyl-HWAHPGGHHA-amide) (Pedersen et al., 2001a), and preliminary AFM data suggest that this transition is related to the formation of a new ripple phase (Pedersen et al., 2001b). Recent AFM measurements concerning the dependence on temperature of the lateral organization of lipid bilayers formed by binary equimolar mixtures of phosphatidylcholines (Kaasgaard et al., 2001)

show that the phase changes (hence transition temperatures) detected by AFM correlate fairly well with the ones related to the thermal anomalies seen in the DSC endotherms of the same system (Leidy et al., 2001). These findings suggest that the combination of the more traditional techniques, such as DSC and NMR (as used in the present investigation together with a model study), with the relatively new AFM technique can serve as a powerful tool for investigating the lateral phase behavior of lipid-peptide systems and for providing accurate temperature-composition phase diagrams.

REFERENCES

Bretscher, M. S., and S. Munro. 1993. Cholesterol and the Golgi apparatus. *Science.* 261:1280–1288.

Cornea, R. L., and D. D. Thomas. 1994. Effects of membrane thickness on the molecular dynamics and enzymatic activity of reconstituted Ca-ATPase. *Biochemistry.* 33:2912–3920.

Datema, K. P., K. P. Pauls, and M. Bloom. 1986. Deuterium nuclear magnetic resonance investigation of the exchangeable sites on Gramicidin A and Gramicidin S in multilamellar vesicles of dipalmitoylphosphatidylcholine. *Biochemistry.* 25:3796–3803.

de Kruijff, B., J. A. Killian, A. G. Rietveld, and R. Kusters. 1997. Phospholipid structure and *Escherichia coli* membranes. *In* Lipid Polymorphism and Membrane Properties. R. M. Epand, editor. Academic Press, San Diego, CA. 477–515.

de Planque, M. R. R., E. Goormaghtigh, D. V. Greathouse, R. E. Koeppe II, J. A. W. Kruijtzer, R. M. J. Liskamp, B. de Kruijff, and J. A. Killian. 2001. Sensitivity of single membrane-spanning alpha-helical peptides to hydrophobic mismatch with a lipid bilayer: effects on backbone structure, orientation, and extent of membrane incorporation. *Biochemistry.* 40:5000–5010.

de Planque, M. R. R., D. V. Greathouse, R. E. Koeppe II, H. Schäfer, D. Marsh, and J. A. Killian. 1998. Influence of lipid/peptide mismatch on the thickness of diacylphosphatidylcholine bilayers: a ^{2}H NMR and ESR study using designed transmembrane α-helical peptides and gramicidin A. *Biochemistry.* 37:9333–9345.

de Planque, M. R. R., J. A. W. Kruijtzer, R. M. J. Liskamp, D. Marsh, D. V. Greathouse, R. E. Koeppe II, B. de Kruijff, and J. A. Killian. 1999. Different membrane anchoring positions of tryptophan and lysine in synthetic transmembrane α-helical peptides. *J. Biol. Chem.* 274: 20839–20846.

Garab, G., K. Lohner, P. Laggner, and T. Farkas. 2000. Self-regulation of the lipid content of membranes by non-bilayer lipids: a hypothesis. *Trends Plant Sci.* 5:489–494.

Gil, T., J. H. Ipsen, O. G. Mouritsen, M. C. Sabra, M. M. Sperotto, and M. J. Zuckermann. 1998. Theoretical analysis of protein organization in lipid membranes. *Biochim. Biophys. Acta.* 1376:245–266.

Greathouse, D. V., R. L. Goforth, T. Crawford, P. C. A. van der Wel, and J. A. Killian. 2001. Optimized aminolysis conditions for cleavage of N-protected hydrophobic peptides from solid phase resins. *J. Peptide Res.* 57:519–527.

Harzer, U., and B. Bechinger. 2000. Alignment of lysine-anchored membrane peptides under conditions of hydrophobic mismatch: a CD, and solid state NMR spectroscopy investigation. *Biochemistry.* 39: 13106–13114.

Huschilt, J. C., R. S. Hodges, and J. H. Davis. 1985. Phase equilibria in an amphiphilic peptide-phospholipid model membrane by deuterium nuclear magnetic resonance difference spectroscopy. *Biochemistry.* 24: 1377–1386.

Ipsen, J. H., G. Karlström, O. G. Mouritsen, H. Wennerström, and M. J. Zuckermann. 1987. Phase equilibria in the phosphatidylcholine-cholesterol system. *Biochim. Biophys. Acta.* 905:162–172.

Jørgensen, K., A. Klinger, and R. L. Biltonen. 2000. Non-equilibrium lipid domain growth in gel-fluid two-phase region of a $DC_{16}PC-DC_{22}PC$ lipid mixture investigated by Monte Carlo simulation, FT-IR, and fluorescence spectroscopy. *J. Chem. Phys. B.* 104:11763–11773.

Kaasgaard, T., C. Leidy, O. G. Mouritsen, J. H. Crowe, and K. Jørgensen. 2001. Real time ripple phase formation in mica supported bilayers visualized by atomic force microscopy. *Biophys. J.* 80:526a. (Abstr.).

Killian, J. A. 1998. Hydrophobic mismatch between proteins and lipids in membranes. *Biochim. Biophys. Acta.* 1376:401–416.

Killian, J. A., and B. de Kruijff. 1985. Thermodynamic, motional, and structural aspects of gramicidin-induced hexagonal H_{II} phase formation in phosphatidylethanolamine. *Biochemistry.* 24:7881–7890.

Killian, J. A., I. Salemink, M. R. R. de Planque, G. Lindblom, R. E. Koeppe II, and D. V. Greathouse. 1996. Induction of non-bilayer structures in diacylphosphatidylcholine model membranes by transmembrane α-helical peptides: importance of hydrophobic mismatch and proposed role of tryptophans. *Biochemistry.* 35:1037–1045.

Killian, J. A., and G. von Heijne. 2000. How proteins adapt to a membrane-water interface. *Trends Biochem. Sci.* 25:429–434.

Kobayashi, Y., and K. Fukada. 1998. Characterization of swollen lamellar phase of dimyristoylphosphatidylcholine-gramicidin A mixed membranes by DSC, SAXS, and densitometry. *Biochim. Biophys. Acta.* 1371:363–370.

Landolt-Marticorena, C., K. A. Williams, C. M. Deber, and R. A. F. Reithmeier. 1993. Non-random distribution of amino acids in the transmembrane segments of human type I single span membrane proteins. *J. Mol. Biol.* 229:602–608.

Leidy, C., T. Kaasgaard, T. V. Ratto, M. Longo, O. G. Mouritsen, J. H. Crowe, and K. Jorgensen. 2001. Lipid domain growth and shape changes as a function of temperature in binary lipid mixtures visualized by atomic force microscopy. *Biophys. J.* 80:1390a. (Abstr.).

Lewis, R. N. A. H., N. Mak, and R. N. McElhaney. 1987. A differential scanning calorimetric study of the thermotropic phase behavior of model membranes composed of phosphatidylcholines containing linear saturated fatty acid chains. *Biochemistry.* 26:6118–6126.

Lindblom, G. 1996. Nuclear magnetic resonance spectroscopy and lipid phase behavior and lipid diffusion. *In* Advances in Lipid Methodology, Vol. 3. W. W. Christie, editor. Oily Press, Dundee, Scotland. 133–209.

Liu, F., R. N. A. H. Lewis, R. S. Hodges, and R. N. McElhaney. 2001. A differential scanning calorimetry and P-31NMR spectroscopy study of the effect of transmembrane alpha-helical peptides on the lamellar-reversed hexagonal phase transition of phosphatidylethanolamine model membranes. *Biochemistry.* 40:760–768.

Loura, L. M. S., A. Fedorov, and M. Prieto. 2000. Partition of membrane probes in a gel/fluid two component lipid system: a fluorescence resonance energy transfer study. *Biochim. Biophys. Acta.* 1467:101–112.

Montecucco, C., G. A. Smith, F. Dabbeni-Sala, A. Johansson, Y. M. Galante, and R. Bisson. 1982. Bilayer thickness and enzymatic activity in the mitochondrial cytochrome c oxidase and ATPase complex. *FEBS Lett.* 144:145–148.

Morein, S., R. E. Koeppe II, G. Lindblom, B. de Kruijff, and J. A. Killian. 2000. The effect of peptide/lipid hydrophobic mismatch on the phase behavior of model membranes mimicking the lipid composition in *Escherichia coli* membranes. *Biophys. J.* 78:2475–2485.

Morein, S., E. Strandberg, J. A. Killian, S. Persson, G. Arvidson, R. E. Koeppe II, and G. Lindblom. 1997. Influence of membrane-spanning α-helical peptides on the phase behavior of dioleoylphosphatidylcholine/water system. *Biophys. J.* 73:3078–3088.

Morrow, M. R., and J. H. Davis. 1988. Differential scanning calorimetry and ^{2}H NMR studies of the phase behavior of gramicidin-phosphatidyl-choline mixtures. *Biochemistry.* 27:2024–2032.

Morrow, M. R., J. H. Davis, F. J. Sharom, and M. L. Lamb. 1986. Studies on the interaction of human erythrocyte band 3 with membrane lipids using deuterium nuclear magnetic resonance and differential scanning calorimetry. *Biochim. Biophys. Acta.* 858:13–20.

Morrow, M. R., J. C. Huschilt, and J. H. Davis. 1985. Simultaneous modeling of phase and calorimetrical behavior in an amphiphilic peptide/phospholipid model membrane. *Biochemistry.* 24:5396–5406.

Mouritsen, O. G. 1990. Computer simulation of co-operative phenomena in lipid membranes. *In* Molecular Description of Biological Membrane Components by Computer Aided Conformational Analysis. R. Brasseur, editor. CRC Press, Boca Raton, FL. 3–83.

Mouritsen, O. G., and M. Bloom. 1984. Mattress model of lipid-protein interactions in membranes. *Biophys. J.* 46:141–153.

Mouritsen, O. G., B. Dammann, H. C. Fogedby, J. H. Ipsen, C. Jeppesen, K. Jørgensen, J. Risbo, M. Sabra, M. M. Sperotto, and M. J. Zuckermann. 1995. The computer as a laboratory for the physical chemistry of membranes. *Biophys. Chem.* 55:55–68.

Mouritsen, O. G., and M. M. Sperotto. 1993. Thermodynamics of lipid-protein interactions in lipid membranes: the hydrophobic matching condition. *In* Thermodynamics of Membrane Receptors and Channels. M. B. Jackson, editor. CRC Press, Boca Raton, FL. 127–181.

Munro, S. 1998. Localization of proteins to the Golgi apparatus. *Trends Cell Biol.* 8:11–15.

Pedersen, T. B., M. C. Sabra, S. Frokjær, O. G. Mouritsen, and K. Jørgensen. 2001a. Association of acylated cationic decapeptides with dipalmitoylphosphatidylserine- dipalmitoylphosphatidylcholine lipid membranes. *Chem. Phys. Lipids.* 113:83–95.

Pedersen, T. B., M. C. Sabra, S. Frokjær, O. G. Mouritsen, and K. Jørgensen. 2001b. Lipid membrane interactions of acylated model peptides. *Biophys. J.* 80:542a. (Abstr.)

Persson, S., J. A. Killian, and G. Lindblom. 1998. Molecular ordering of interfacially located tryptophan analogs in ester- and ether-lipid bilayers. *Biophys. J.* 75:1365–1371.

Peschke, J., J. Riegler, and H. Möhwald. 1987. Quantitative analysis of membrane distortions induced by mismatch of protein and lipid hydrophobic thickness. *Eur. Biophys. J.* 14:385–391.

Pink, D. A., J. G. Green, and D. Chapman. 1980. Raman scattering in bilayers of saturated phosphatidylcholines: experiment and theory. *Biochemistry.* 19:349–356.

Reithmeier, R. A. F. 1995. Characterization and modeling of membrane proteins using sequence analysis. *Curr. Opin. Struct. Biol.* 5:491–500.

Ridder, A. N. J. A., S. Morein, J. G. Stam, A. Kuhn, B. de Kruijff, and J. A. Killian. 2000. Analysis of the role of interfacial tryptophan residues in controlling the topology of membrane proteins. *Biochemistry.* 39:6521–6528.

Riegler, J., and H. Möhwald. 1986. Elastic interactions of photosynthetic reaction center proteins affecting phase transitions and protein distributions. *Biophys. J.* 49:1111–1118.

Rinia, H. A., J.-W. Boots, D. T. S. Rijkers, R. A. Kik, R. A. Demel, M. M. E. Snel, J. A. Killian, J. P. J. M. van der Eerden, and B. de Kruijff. 2002. Anchoring residue specific domain formation by transmembrane peptides in gel-state phospholipid bilayers. *Biochemistry.* In press.

Rinia, H. A., R. A. Kik, R. A. Demel, M. M. E. Snel, J. A. Killian, J. P. J. M. van der Eerden, and B. de Kruijff. 2000. Visualization of highly ordered striated domains induced by transmembrane peptides in supported phosphatidylcholine bilayers. *Biochemistry.* 39:5852–5858.

Rouser, G., S. Fleischer, and A. Yamamota. 1970. Two-dimensional thin layer chromatographic separation of polar lipids and determination of phospholipids by phosphorous analysis of spots. *Lipids.* 5:494–496.

Seelig, J. 1978. Phosphorous-31 nuclear magnetic resonance and the head-group structure of phospholipids in membranes. *Biochim. Biophys. Acta.* 505:105–141.

Segrest, J. P., H. De Loof, J. A. Dohlman, C. A. Brouillette, and A. M. Anantharamanah. 1990. Amphipathic helix motif—Classes and properties. *Proteins Struct. Funct. Genet.* 8:103–117.

Silvius, J. R. 1982. Thermotropic phase transitions of pure lipids in model membranes and their modification by membrane proteins. *In* Lipid-Protein Interactions, Vol. 2. P. C. Jost and O. H. Griffith, editors. Wiley-Interscience, New York, NY. 239–281.

Sperotto, M. M. 1997. A theoretical model for the association of amphiphilic transmembrane peptides in lipid bilayers. *Eur. Biophys. J.* 26:405–416.

Sperotto, M. M., J. H. Ipsen, and O. G. Mouritsen. 1989. Theory of protein-induced lateral phase separation in lipid membranes. *Cell Biophys.* 14:79–95.

Sperotto, M. M., and O. G. Mouritsen. 1988. Dependence of lipid membrane phase transition temperature on the mismatch of protein and lipid hydrophobic thickness. *Eur. Biophys. J.* 16:1–10.

Van der Wel, P. C. A., T. Pott, S. Morein, D. V. Greathouse, R. E. Koeppe II, and J. A. Killian. 2000. Tryptophan-anchored transmembrane peptides promote formation of nonlamellar phases in phosphatidylethanolamine model membranes in a mismatch-dependent manner. *Biochemistry.* 39:3124–3133.

Vist, M. R., and J. H. Davis. 1990. Phase equilibria of cholesterol/dipalmitoylphosphatidylcholine mixtures: ^{2}H nuclear magnetic resonance and differential scanning calorimetry. *Biochemistry.* 29:451–464.

von Heijne, G. 1994. Membrane proteins: from sequence to structure. *Annu. Rev. Biophys. Biomol. Struct.* 23:167–192.

Wallin, E., T. Tsukihara, S. Yoshikawa, G. von Heijne, and A. Elofsson. 1997. Architecture of helix-bundle membrane proteins: an analysis of cytochrome c oxidase from bovine mitochondria. *Protein Sci.* 6:808–815.

Yau, W.-M., W. C. Wimley, K. Gawrish, and S. H. White. 1998. The preference of tryptophan for membrane interfaces. *Biochemistry.* 37:14713–14718.

Zhang, Y.-P., R. N. A. H. Lewis, G. D. Henry, B. D. Sykes, R. S. Hodges, and R. N. McElhaney. 1995a. Peptide models of helical hydrophobic transmembrane segments of membrane proteins. 1. Studies of conformation, intrabilayer orientation, and amide hydrogen exchangeability of Ac-K$_2$-(LA)$_{12}$-K$_2$-amide. *Biochemistry.* 34:2348–2361.

Zhang, Y.-P., R. N. A. H. Lewis, R. S. Hodges, and R. N. McElhaney. 1992. Interaction of a peptide model of a hydrophobic transmembrane α-helical segment of a membrane protein with phosphatidylcholine bilayers: differential scanning calorimetric and FTIR spectroscopic studies. *Biochemistry.* 31:11579–11588.

Zhang, Y.-P., R. N. A. H. Lewis, R. S. Hodges, and R. N. McElhaney. 1995b. Peptide models of helical hydrophobic transmembrane segments of membrane proteins. 2. Differential scanning calorimetric and FTIR studies of the interaction of Ac-K$_2$-(LA)$_{12}$-K$_2$-amide with phosphatidylcholine bilayers. *Biochemistry.* 34:2362–2371.

Zhang, Z., M. M. Sperotto, M. J. Zuckermann, and O. G. Mouritsen. 1993. A microscopic model for lipid/protein bilayers with critical mixing. *Biochim. Biophys. Acta.* 1147:154–160.